

## A laser diode/HOE pattern recognition system

DAVID CASASANT, M. SHEN\*, F. CAIMI, T. LUU AND B. FENG\*

(Department of Electrical Engineering, Carnegie-Mellon University Pittsburgh, PA 15213)

(Received 9 September 1980)

### Abstract

A compact and rugged optical correlator is described. It employs a lensless matched spatial filter that is formed at one wavelength. Correlation is performed with a laser diode at a second wavelength using an imaging lens in a scaling correlator topology.

### 1. Introduction

Optical pattern recognition by matched spatial filter (MSF) correlation<sup>[1]</sup> is a well-known technique. The advent of holographic optical elements (HOEs)<sup>[2,3]</sup>, laser diode sources and new architectures has made rugged and compact versions of such systems most attractive<sup>[4~7]</sup>. Such systems are useful for both commercial and airborne applications. In this paper we provide the first discussion unifying all aspects of a laser diode/HOE correlator system. Theoretical analysis, experimental data and the results of several correlations performed on the system are provided.

A lensless MSF system<sup>[7~9]</sup> used to reduce component positional requirements is described in sect. 2. Correlation experiments are provided to show that HOE aberrations are reduced by weighted MSF synthesis<sup>[10]</sup>. The wavelength scaling correlator in sect. 3 is necessary to permit correlation at one wavelength and MSF synthesis at another wavelength. This is necessary when a laser diode source is used. In sect. 4, the full system is shown and its performance discussed.

### 2. Lensless MSF/HOE

The system used to record a lensless MSF is shown in Fig. 1. It is similar to the conventional technique<sup>[1]</sup> except for the use of a converging reference beam. With  $h(x_1)$  placed at  $P_1$ , its Fourier transform (FT)  $H(x_2)$  is formed at  $P_2$  and the term of interest in the MSF pattern at  $P_2$  is

$$u_t(x_2) = H^*(x_2/\lambda f_L) \exp[-jk(x_0 - x_2)^2/2z], \quad (1)$$

where all parameters are defined in Fig. 1. From (1) we see that the MSF also contains

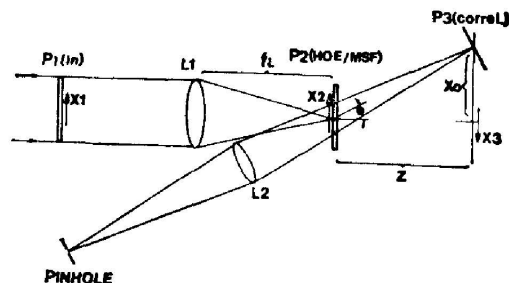


Fig.1 Schematic diagram of a lensless MSF optical correlator system<sup>[15]</sup>

\* Visiting Scholars from Institute of Optics and Electronics, Academia Sinica, PRC.

the transfer function of an FT lens. Thus if  $h(x_1)$  is repositioned in  $P_1$  and the reference beam is blocked, the  $P_2$  recording will focus a point of light at  $x_3 = x_0$  whose location shifts about  $x_0$  as the position of  $h$  in  $P_1$  shifts from its original position.

By recording such an MSF, the length and complexity of the system are reduced, so no positional tolerances exist between  $P_2$  and  $P_3$  since no discrete second FT lens exists. Many versions of such a system have been suggested<sup>[11~14]</sup>, none for the use we consider.

The system of Fig. 1 was assembled using:  $\lambda = 633 \text{ nm}$ ,  $f_L = 500 \text{ mm}$ ,  $\theta = 11.3^\circ$  and  $x_0 = 78 \text{ mm}$ . The input function  $f$  used is shown in Fig. 2a. It contains four occurrences of the key word "PROFESSOR", which we select as our reference function  $h$  (Fig. 2b). A lensless MSF of this function  $h$  was produced at  $P_2$ . When  $f$  was placed at  $P_1$ , the output correlation plane pattern in the vicinity of  $(x_3, y_3) = (x_0, 0)$  in  $P_3$  appeared as shown in Fig. 2c on an isometric display. Four correlation peaks are observed and their locations are seen to correspond to the four occurrences of the reference word in the full input image<sup>[15]</sup>.

A feature of this and any MSF optical pattern recognition system is proper selection of the beam balance ratio  $K = |u_r/u_s|^2$  used during MSF synthesis<sup>[10]</sup>. Since  $u_s$  varies spatially, so does  $K$ . Since the modulation of the MSF is a maximum when  $K = 1$ , we can select the spatial frequency band in which to set  $K = 1$  and hence enhance certain

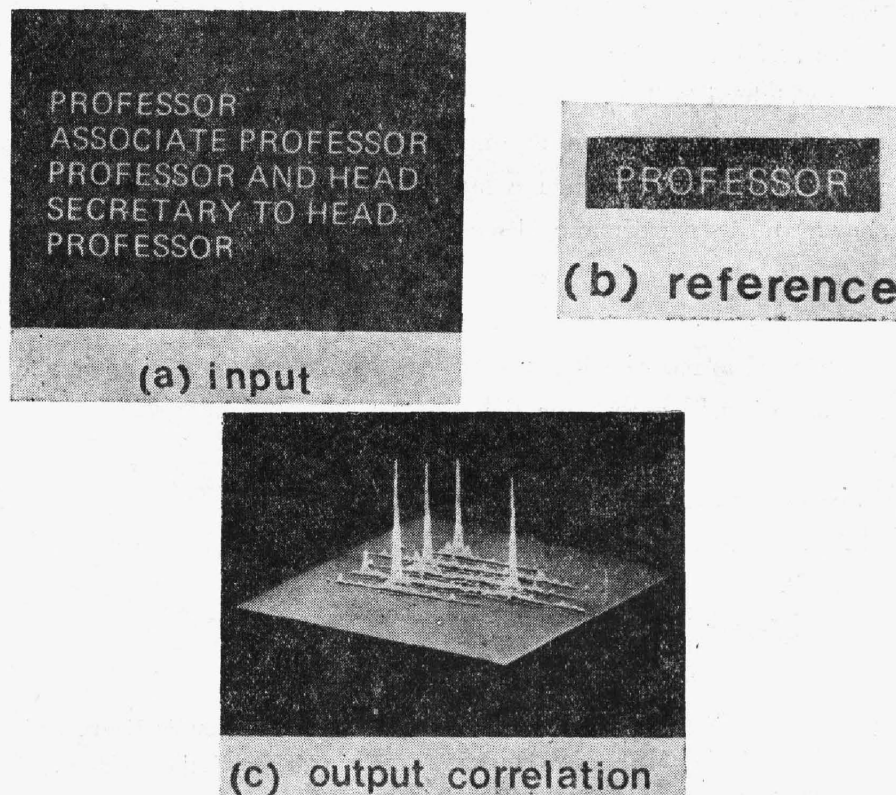


Fig.2 Optical pattern recognition performed on the system<sup>[15]</sup>

spatial frequencies in the input data during MSF synthesis. We refer to this as weighted MSF synthesis<sup>[10]</sup>. For the input text data of Fig. 2a, we set  $K=1$  at spatial frequencies corresponding to the width and half-height of a letter. This bandpass filtered text data requires the HOE to operate over a reduced spatial frequency range, thus greatly improving aberrations as we now discuss.

In the design of this system and experiment, particular attention was given to astigmatic aberrations since this is one of the major error sources in such a system<sup>[9,16]</sup>. We include only third order aberrations, denote the field angle of the key object by  $\tan\beta = \varepsilon/f_1$  and assume  $\tan\beta \ll 2x_0/R_0$ , where  $R_0$  is the distance from the center of  $P_2$  to  $x_3 = x_0$ . We then find the optical path difference for the system to be  $\Delta r_a \simeq x_0^2 (\tan\beta) / R_0^2$ . For an input aperture  $D$ , we find  $(\tan\beta)_{\max} = D/2f_L$ . If the maximum input spatial frequency is  $f_m$ , then the maximum optical path difference error is

$$\Delta r_{a \max} = f_m^2 \lambda^2 D f_L \sin\theta / 2R_0, \quad (2)$$

where  $\sin\theta = x_0/R_0$ . In the design of our experimental system, we restricted  $f_m$  and  $D$ , minimized  $\theta$  and  $f_L$ , while increasing  $R_0$  to maintain large output correlation peak intensities. To determine the amount of  $I_p$  loss to be expected for a given translation of the input, we used the astigmatic wave aberration equations of Champagne<sup>[16]</sup> and found the phase aberration due to astigmatism for the system of Fig. 1 to be

$$\phi_a = K x_n^2 s_0 \Delta x_3 / R_0^3, \quad (3)$$

where  $x_n$  is the aperture of the HOE. The shift  $\Delta x_3$  in the location of the correlation peak is related to the corresponding shift  $\Delta x_1$  of  $h$  in the input by  $\Delta x_3 = R_0 \Delta x_1 / f_L = 0.8 \Delta x_1$  for our experimental system. The maximum MSF aperture is  $2x_0 = 7.88$  mm from before.

Using these values in the quadratic phase model  $\phi_a = B x_n^2$ , where  $x_n = x_n/x_0$ , we find  $B = 1.6\pi x_0^2 \Delta x / \lambda R_0^3$ . Following<sup>[17]</sup>, we estimate the correlation peak intensity as a function of the lens phase error  $\phi_a$  by  $p = 1 - \sigma_\phi^2 = 1 - 4B^2/45$ , where  $\sigma_\phi$  is the standard deviation of  $\phi_a$  over the full aperture. A theoretical plot of  $p$  versus  $\Delta x_1$  is shown in Figure 3 for the experimental system used. From this plot, we see that input displacements of  $\pm 10$  mm should result in a theoretical loss in output  $I_p$  of only 20%.

Experimental verification of this equation (Fig. 3) showed only 10% loss in  $I_p$ . Since the above phase error model assumes the aberrations to exist over the entire 25 cy/mm HOE aperture, whereas the weighted MSF band-passed only the region above 3.7 cy/mm,

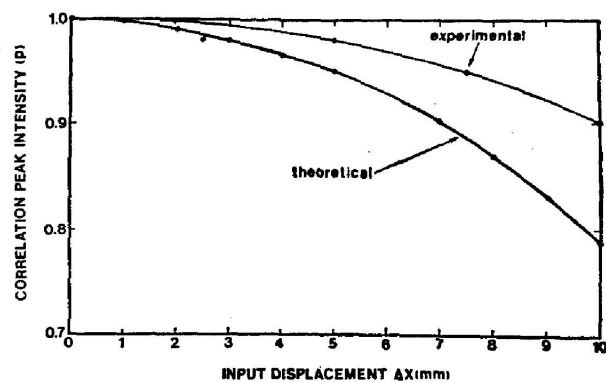


Fig.3 Theoretical and experimental graph of correlation peak intensity versus input displacement for the experiment in Fig. 2 on the system in Fig. 1<sup>[15]</sup>

our experimental performance is expected to be superior to that predicted by theory.

### 3. Wavelength-scaling correlator

We next consider the off-line synthesis of the lensless MSF at one wavelength ( $\lambda_1$ ) and its subsequent use in a correlator illuminated with a second wavelength ( $\lambda_2$ ) of light. Such a case arises when a laser diode is used as the light source during correlation. Since MSF materials of adequate holographic quality are not available with good response in the normal wavelength ranges of laser diodes, off-line filter synthesis with a gas laser is necessary. Correlation with a laser diode then follows. The final system is shown in Fig. 4. The input is placed behind the lens a distance  $d$  from the MSF plane. As the distance  $d$  is varied, the size of the FT is scaled by  $f_L/d$ . Such a wavelength scaling correlator is needed to compensate for the  $\mu = \lambda_2/\lambda_1 \neq 1$  wavelength change. This system also results in lower aperture and spatial frequency requirements for HOE 1, thus decreasing its aberration effects.

A modified version Fig. 4 was assembled<sup>[18]</sup> to verify performance of the idea using

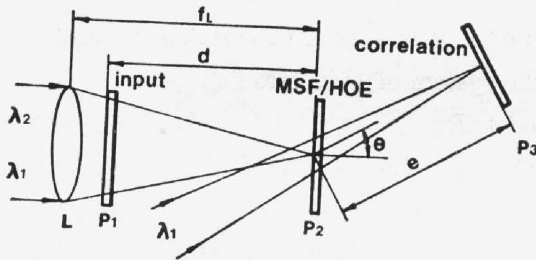


Fig.4 Schematic diagram of a laser diode/lensless MSF correlator<sup>[7]</sup>

a collimated gas laser ( $\lambda_2 = 633 \text{ nm}$ ) in place of the laser diode and a second laser source ( $\lambda_1 = 488 \text{ nm}$ ) to form the lensless MSF/HOE at  $P_2$ . After the MSF was formed at  $\lambda_1$  as before, the reference beam was blocked and the  $\lambda_2$  source used to illuminate the input. To properly scale and match the FT of the input to that of the reference, we adjusted the distances

to satisfy  $d_2 = \lambda_1 d_1 / \lambda_2$  and  $e_2 = e_1 / \mu$ , where  $\mu = 1.3$  ( $d_2$  and  $e_2$  are distances used during correlation while  $d_1$  and  $e_1$  are the corresponding distances used during MSF synthesis).

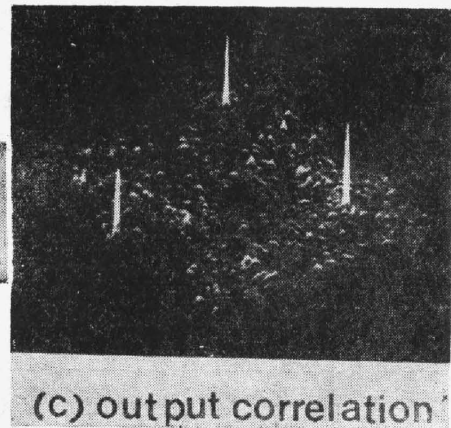
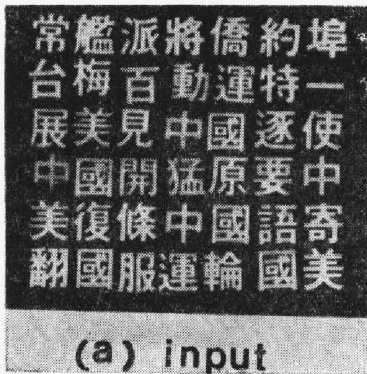


Fig.5 Experimental image pattern recognition data obtained using a modified versions of the system in Fig. 4

It was also necessary to adjust  $\theta$  to satisfy  $\sin \theta_1 = \mu \sin \theta_2$ . We kept  $\Delta x_1 \ll d_2$  and  $\Delta x_3 \ll e_2$  to reduce field angles and HOE aberrations.

The system was assembled with  $e_1 = d_1 = 400$  mm and  $\theta_1 = 17^\circ$  and correlations were successfully obtained (see Fig. 5) using weighted MSF synthesis as before. Good shift invariance ( $\leq 10\%$  variation in SNR for  $\pm 10$  mm input displacements) was again obtained. The experiments were repeated with both a glass and an HOE lens for  $L_1$ . Slightly lower correlation SNR values were obtained in the second case due to the low  $\eta = 3\%$  of the HOEs used (dichromated gelatin or bleached HOEs would yield larger  $\eta = 80\%$  levels). System variations such as these and others are possible but not needed for our application.

#### 4. Laser diode correlator

As noted at the outset, the major motivation for this study was the use of a lensless HOE/MSF (synthesized off-line with a gas laser) in a correlator using a laser diode source. We now consider such a laser diode/lensless MSF system of Fig. 4 with  $\lambda_1 = 633$  nm (He-Ne laser),  $\lambda_2 = 794.5$  nm (ML-4001 laser diode),  $e_1 = d_1 = 400$  mm,  $f_{L1} = 760$  mm, a maximum input spatial frequency  $f_m = 10$  cy/mm, a maximum MSF aperture  $x_m = 2.5$  mm, an input aperture of half width  $\Delta x_1 = 12.5$  mm, and a displacement  $x_0 = 100$  mm of the center of  $P_3$  from the optical axis. With these system parameters, the astigmatic aberration equation of Champagne<sup>[16]</sup> (using our notation) becomes

$$W_a = (x_m^2/2\lambda_2) [(\mu^3 - \mu)x_0^2/e_1^3 + 2\mu^3 x_0 \Delta x_1/e_1^2 d_1 + (\mu^3 \Delta x_1^2/d_1^2)(1/e_1 - 1/d_1)]. \quad (4)$$

For our system parameters, quite good maximum and rms astigmatism value were obtained:  $(W_a)_{\max} = 0.44 \lambda_2$  and  $(W_a)_{\text{rms}} = 0.13 \lambda_2$ . Weighted MSF synthesis will make the effective  $W_a$  even less (as shown in sect. 2).

The temporal coherence of a laser diode is another source of concern. It varies with power and temperature producing a spectral source width  $\Delta \lambda_2$  that will limit<sup>[41-7]</sup> the useable linear 1-D input space-bandwidth  $N$ , to

$$N \leq \lambda_2 / \Delta \lambda_2, \quad (5)$$

or reciprocal of the fractional wavelength change.

For the ML-4001 single-mode Mitsubishi laser diode used,  $\Delta \lambda_2 = 0.2$  nm is specified. Temperature effects can be expected to shift the source's wavelength by a maximum of  $\Delta \lambda_2 = 2$  nm, in which case  $N$  should be restricted to 400 points per line. This is less than 512 line television resolution, but the above analysis is worse-case, since considerable spatial frequency data below the maximum is usually the major contribution to the correlation.

The source's spectral width  $\Delta \lambda_2$  also produces a divergence  $\Delta \theta_2$  in the wavefront leaving  $P_2$  during correlation and hence affects the shape of the correlation peak. To reduce the effects of  $\Delta \lambda_2$  on the drop of the correlation peak, we require

$$\Delta\lambda_2 \leq \lambda_2^2 / (2\mu x_m \sin \theta_1). \quad (6)$$

For our system,  $x_m = 2.5$  mm,  $\sin \theta_1 = 0.25$ ,  $\mu = 1.26$ ,  $\lambda_2 = 795.4$  nm and the spectral width of the source should thus be less than 0.4 nm. A change in device temperature will result in a wavelength shift rather than an increase in the spectral width of the source. Only the  $\Delta\lambda$  spread (rather than the  $\lambda_2$  shift) affects the shape of the correlation peak. Since the specified  $\Delta\lambda_2 = 0.2$  nm for the laser diode used is less than the above requirement of 0.4 nm, no problem is foreseen in this regard with our indicated design. The spatial coherence of the laser diode source was also considered and found to be quite good with less than a 1.2 dB variation in correlation SNR expected for the maximum input shifts.

Another concern in the use of a laser diode is proper source collimation. If the entire aperture angle of the laser diode is  $2u = 10^\circ$  (see Fig. 4) and the wavelength of the laser diode is  $0.795 \mu\text{m}$ , then the main lobe due to aperture diffraction will have a width of  $4.6 \mu\text{m}$ . Therefore, the small ( $1 \sim 2 \mu\text{m}$ ) emission area of the laser diode used allows us to consider it as a point source, that is more or less equivalent to the diffraction limit of the optical system. The above example also indicates that the aperture angle from the laser diode should be restricted to some degree.

In the laser diode scaling-correlation system in Fig. 4, a suitable convergent coherent beam incident on  $P_1$  is needed whether the beam is parallel or not before the first Fourier transform lens. The convergence angle of the laser diode and the above diffraction limited resolution analysis enable us to use the simple imaging optical system shown for  $L_1$  in Fig. 4. Lens  $L_1$  then requires quite modest specifications. It could be a simple cemented doublet, which can be corrected for spherical aberration. We thus obtain the greatly simplified and compact correlator shown that uses one glass imaging lens and a HOE/MSF element.

Since the radiant intensity distribution of a laser diode is different in orthogonal directions, some added attention is needed to lens system  $L_1$ . As the distance from  $L_1$  to the source is increased (i. e. the aperture angle  $u$  is decreased), the illumination of  $P_1$  will become more uniform but less light power will enter the input aperture. We must thus make a choice between the uniformity of illumination and the power that can be used in selecting the distance from source to  $L_1$  and the aperture angle  $u$ .

For the ML-4001 laser diode, its full irradiance angle at half power was  $10^\circ$  (vertical) and  $40^\circ$  (horizontal). We assume a Gaussian intensity distribution for the light. Then the light intensity  $I_u$  at the aperture is

$$I_u = I_0 \exp(-u^2/2\sigma^2), \quad (7)$$

where  $I_0$  is the intensity at the center of the aperture and  $\sigma$  is the standard deviation. In the more critical direction (vertical),  $I_u = 0.5I_0$  when  $u = 5^\circ$  and then  $\sigma = 4.25^\circ$ . We chose the spacing from  $L_1$  to the source to intercept a  $7^\circ$  cone angle subtended by the input aperture. For this system,  $u = 3.5^\circ$  and only one-sixth of the light from the source

is used. Using (7) we find  $I_u = 0.7I_0$  at the edges of the  $P_1$  aperture. This indicates that the ratio of the correlation peak intensity at the center and edge of the plane will be 0.7 or only about 1.5 dB.

Both spatial coherence and uniformity of illumination will affect the system's shift-invariance, i. e. the variation in  $I_p$  and SNR with location of the correlation peak. For the system design chosen, the effects of spatial coherence and uniformity of illumination are nearly equal (each results in a 1.2~1.5 dB maximum  $I_p$  and SNR loss).

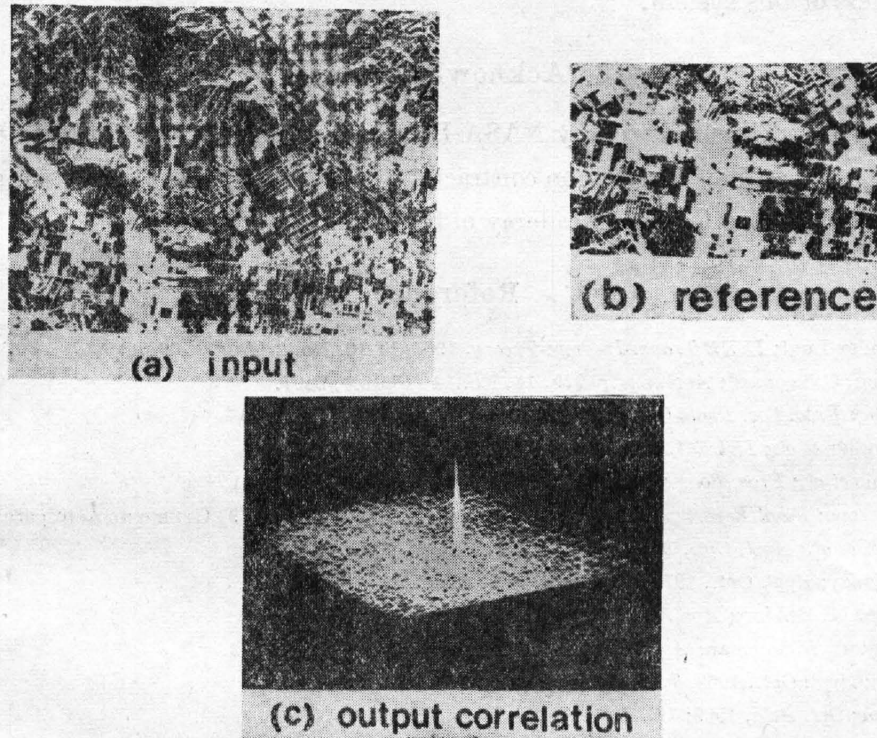


Fig.6 Experimental image pattern recognition data obtained using the system in Fig. 4.<sup>[7]</sup>

All the above analysis issues were incorporated into the design of an experimental system in the topology of Fig. 4. In Fig. 6 we show the input, reference and output correlation plane pattern obtained with the MSF formed at  $\lambda_1 = 488$  nm and correlation performed with a laser diode at  $\lambda_2 = 795.4$  nm. The input transparency used was a radar image with a 24 mm  $\times$  30 mm format. The SNR of the correlation is quite good as shown even though the reference was located at the edge of input scene.

## 5. Summary and conclusions

A small size and weight optical correlator suitable for airborne applications has been described, designed, analyzed, fabricated, tested and successfully demonstrated. The system employs holographic optical elements in a lensless MSF architecture with

improved system alignment and stability features. The light source used during correlation was a laser diode. It was thus necessary to record the matched spatial filter at one wavelength and perform the correlation at the different wavelength of the laser diode. A scaling correlator architecture was used to accommodate the wavelength change and a simple imaging input lens is needed to focus the laser diode onto the filter. A complete system design and analysis including aberration effects and with attention to the system's shift-invariance was performed. The experimental results obtained verified the usefulness of this system.

## 6. Acknowledgements

The support of this research by NASA Langley on contract NAS1-16125 and the Air Force Office of Scientific Research on contract AFOSR-79-0091 is gratefully acknowledged as is the support of the Chinese Academy of Sciences.

## Reference

- [ 1 ] A. Vander Lugt; *IEEE Trans. Inform. Theory*, 1964, **IT-10**, No. 2 (Apr), 139.
- [ 2 ] B. Chang, C. Leonard; *Appl. Opt.*, 1979, **18**, No. 14 (15 Jul), 2407.
- [ 3 ] B. Chang; *Proc. Soc. Photo-Opt. Instrum. Engrs*, 1979, **177**, 71.
- [ 4 ] B. Guenther *et al.*; *IEEE J. Q. E.*, 1979, **QE-15**, No. 12 (Dec), 1348.
- [ 5 ] J. Duthie *et al.*; *Proc. Soc. Photo-Opt. Instrum. Engrs*, 1980 (Apr), **231**.
- [ 6 ] C. Calderone; *Final Report on Contract DAAK 40-77-6-0089* (17 Dec 1979), Grumman Aerospace Corporation.
- [ 7 ] F. Caimi *et al.*; *Appl. Opt.*, 1980, **19**, No. 16 (15 Aug), 2653.
- [ 8 ] W. Maloney; *Appl. Opt.*, 1971, **10**, No. 9 (Sep), 2127.
- [ 9 ] M. Bage, M. Beddoes; *Appl. Opt.*, 1976, **15**, No. 11 (Nov), 2830.
- [10] D. Casasent, A. Furman; *Appl. Opt.*, 1977, **16**, No. 6 (Jun), 1652, 1662.
- [11] G. Groh; *Appl. Opt.*, 1968, **7**, No. 8 (Aug), 1643.
- [12] D. Gabor; *Opt. Acta*, 1969, **16**, No. 4 (Jul-Aug), 519.
- [13] S. Ragnarsson; *Phys. Scr.*, 1970, **2**, No. 4~5, 145.
- [14] R. Binns; *Appl. Opt.*, 1968, **7**, No. 6 (Jun), 1047.
- [15] M. Shen *et al.*; *Opt. Commun.*, 1980, **34**, No. 3 (Sep), 311.
- [16] E. Champagne; *J. O. S. A.*, 1967, **57**, No. 1 (Jan), 51.
- [17] T. Luu, D. Casasent; *Appl. Opt.*, 1979, **18**, No. 6 (15 Mar), 791.
- [18] M. Shen *et al.*; *Opt. Commun.*, 1980, **34**, No. 3 (15 Mar), 316.



# 应用激光二极管和全息元件的 光学图象识别系统

DAVID CASSASANT, F. CAIMI and T. LUU

(*Department of Electrical Engineering, Carnegie-Mellon University*)

沈忙作\* 冯伯儒\*

(中国科学院光电研究所)

## 提 要

在光学信息处理中,用匹配空间滤波器可以进行图象识别和定位的运算。全息光学元件(HOE)以及激光二极管的出现,使得研制结构紧凑而稳定的光学图象识别系统有了可能。这样的识别系统对航天和机载的应用有重要的意义。本文首次和比较全面地从理论和实验的角度论述了整个应用激光二极管和全息元件的图象识别系统。

该系统采用了无透镜匹配空间滤波器。这就是用全息透镜代替一般相关器中的第二傅里叶变换透镜,并且把它与匹配空间滤波器综合在一张全息干板上。结果,简化了系统的结构,提高了稳定性,避免了滤波器与第二傅里叶变换透镜相对位置的调整问题。

本文首先从理论的角度分析了这一系统的可行性,指出在输出平面可以获得相关结果,相关峰值位置对应于输入图象的相对位置(位移不变性),并且用实验证实了这一结果。由于参考光束有一定的倾斜角,综合在匹配滤波器上的实际是一个离轴全息透镜,轴外象差(特别是象散)应加以限制。本文列出了该系统三级象散的计算公式,用实例估算了象散的大小,说明只要合理选择系统参数,象差可控制在允许的范围内,保证输出相关亮点不致扩散。

目前的激光二极管发射的激光相干长度短,波长较长,功率不够大,所以只能用于相关识别,同时制作匹配滤波器还必须用常用的气体激光器。因而记录与识别之间,存在波长改变的问题。为适应波长的变化,系统的某些参数要作相应的变更。我们采用了变比例相关器,维持匹配空间滤波器上空间频率比例因子不变。我们用氩离子激光器制作滤波器,用氦氖激光器相关,实验证明改变波长是现实的。

用激光二极管做光源,波长的变化使象散有所增加,其计算公式将不同于单色光象散公式。计算表明,用激光二极管时,所用的系统能够满足要求。

激光二极管所发射激光的单色性要比一般的气体激光低,它限制了输入信号的空间带宽积。单色性的另一影响是使相关输出脉冲加宽,峰值下降。分析计算说明,现有的激光二极管已能满足每帧 512 行电视信号的要求和相关脉冲宽度的要求。

收稿日期: 1980 年 9 月 9 日

\* 现在 Carnegie-Mellon University 访问研究

实验表明, 二极管激光的空间相关性影响视场边缘的相关峰值强度。文中介绍了测量空间相关性的方法以及空间相关性与相关峰值强度的关系。

激光二极管有显著的方向性, 在不同的方向上, 发射强度差别较大, 造成输出视场中相关峰值强度的变化。因此在系统设计时, 要合理选择准直物镜的参数, 兼顾输入视场照明均匀和有效利用激光功率的要求。

文中最后介绍了一个应用激光二极管和全息元件的图象识别系统和它的实验结果。该系统中除了输入和输出平面外, 一共只有一个二极管激光器, 一个玻璃准直透镜和一块全息滤波器, 这是到目前为止最简单、最紧凑的相关器。

